Pergamon

Geochimica et Cosmochimica Acta, Vol. 68, No. 9, pp. 2119–2128, 2004

0016-7037/04 $30.00 + .00

doi:10.1016/j.gca.2003.10.038

Chemistry and mineralogy of ochreous sediments in a constructed mine drainage wetland

W. B. Gagliano,[1,*] M. R. Brill,[1] J. M. Bigham,[1] F. S. Jones,[1] and S. J. Traina[2]

[1]School of Natural Resources, The Ohio State University, 2021 Coffey Road, Columbus, OH 43210, USA
[2]Sierra Nevada Research Institute, University of California, Merced, P.O. Box 2039, Merced, CA 95344, USA

(*Received October* 16, 2002; *accepted in revised form October* 6, 2003)

Abstract—The objective of this study was to examine the mineralogy and geochemical stability of ochreous sediments accumulated in a compost wetland constructed in 1990 for acid mine drainage treatment. Intact sediment cores were collected in 1996 and 2000 from an area that had accumulated 33 cm of ochre. Solids and pore waters were subsequently separated by centrifugation and analyzed using conventional methods, including X-ray diffraction, infrared spectroscopy, scanning electron microscopy, and wet chemical techniques. The solid phase had an average Fe content of 585 g/kg and was predominantly schwertmannite [$Fe_8O_8(OH)_{4.8}(SO_4)_{1.6}$] in the upper portion of the sediment column, but transformed to goethite (α-FeOOH) with depth. The rate of transformation was calculated to be 30 mol/m^3/yr in the initial 6 yr of sedimentation as compared to 10 mol/m^3/yr for the 4-yr period from 1996 to 2000. Pore water composition was affected by this mineral transformation through production of acidity and the release of Fe and SO_4. These results demonstrate that the sediment column was not a static environment. In addition, the transformation of schwertmannite to goethite, which has been observed under laboratory conditions, also occurs in natural systems.

1. INTRODUCTION

Drainage from coal mines has resulted in a severe water quality problem for the eastern United States. The oxidation of sulfide minerals in coals and associated rocks releases iron-rich, acidic solutions that may contain elevated levels of trace metals (Winland et al., 1991; Hyman and Watzlaf, 1997; Rose and Cravotta, 1998; Nordstrom and Alpers, 1999). When mine drainage enters natural waterways, changes in pH and the formation of ochreous precipitates can have devastating effects on aquatic ecosystems.

Mine drainage may persist for decades, making it a challenging problem to address. Treatment methods often involve the addition of alkaline reagents that neutralize acidity and precipitate dissolved metals (Skousen, et al., 1998). These methods are effective but require continuous oversight and a large investment of resources. More recently, constructed wetlands have been implemented as a low-maintenance, cost-effective means of achieving long-term treatment of mine drainage (Hedin et al., 1994). The specific design parameters and technology implemented in these wetlands varies with drainage quality and local site conditions, but a common feature is their function as a reservoir for secondary iron precipitates (Hedin et al., 1994; Skousen et al., 1998; Barton and Karathanasis, 1999).

The iron precipitates from mine drainage include a variety of poorly ordered oxides and hydroxysulfates that are effective sorbents of trace metals and oxyanions (Karathanasis and Thompson, 1995; Webster et al., 1998; Bigham and Nordstrom, 2000). The geochemical stability of these iron precipitates and their associated contaminant loads are an issue because poorly ordered minerals such as ferrihydrite ($HFe_5O_8{\cdot}4H_2O$) and schwertmannite [$Fe_8O_8(OH)_6SO_4$] spontaneously transform with time into more stable minerals, such as goethite (α-FeOOH), that may be less efficient sorbents of contaminants (Bigham et al., 1996; Rose and Ghazi, 1997; Desborough et al., 2000). This transformation process may be accelerated by the development of pH or redox gradients within the sediment column of lakes (Peine et al., 2000), reservoirs, or wetlands receiving mine drainage. Such conditions could facilitate the dissolution of iron precipitates or desorption of metals resulting in a latent source of pollution. The objective of this study was to determine the mineralogy of ochreous precipitates and quantify rates of mineral transformation in the sediment column of a wetland receiving acid mine drainage.

2. MATERIAL AND METHODS

2.1. Field Site Description and Sampling

The field site used in this study was a wetland constructed for mine drainage treatment near Carbondale in Athens County, Ohio. This wetland was established in 1990 and consists of a series of six rectangular sedimentation cells, each approximately 1020 m^2, followed by a deeper pond covering a total area of over 6000 m^2 (Fig. 1). The sedimentation cells were clay lined, layered with 30 cm of limestone substrate and 38 cm of compost material (either spent mushroom or manure compost), and planted initially with cattails (*Typha spp.*) at a density of 17 plants per m^2. Each cell was divided into thirds by two retaining boards to distribute the drainage water evenly, prevent short circuiting, and maintain a water depth of ~10 cm.

Multiple sediment cores were collected during 1996–1997 and 2000–2001 using clear plastic cylinders that were 7 cm in diameter and approximately 70 cm in length. Each cylinder was pushed into the sediment column, a stopper was placed on top to create a vacuum, the core was gently withdrawn, and a second stopper was placed in the bottom to retain the sediment. The sediment cores were transported on ice to the laboratory where they were extruded from the tubes under flowing Ar and divided into segments of 3–4 cm length or corresponding to visual banding patterns. The segments of sediment were then transferred to 250-mL centrifuge bottles under Ar and centrifuged for 15 min at 9100 RCF to separate pore waters from the solids for prompt geochemical and mineralogical analyses, respectively. The data pre-

* Author to whom correspondence should be addressed (gagliano.4@osu.edu).

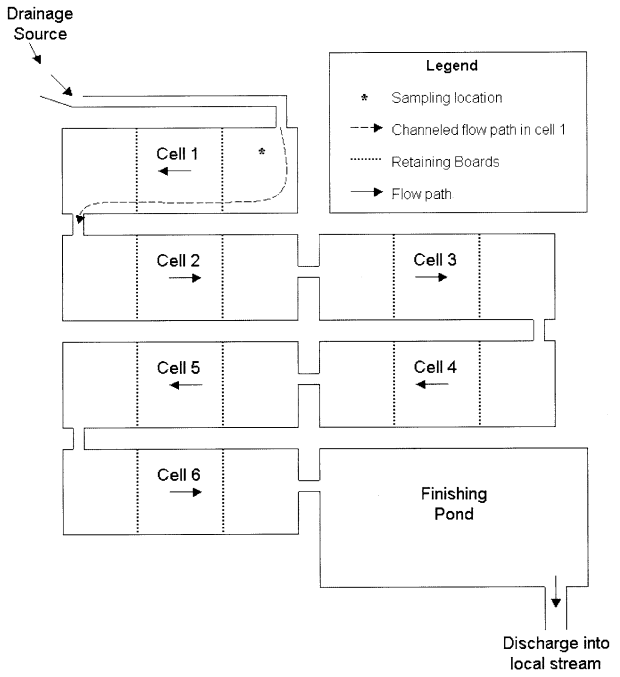

Fig. 1. Schematic diagram of the Carbondale wetland.

sented in this paper are from cores collected on September 17, 1996 and October 21, 2000 near the inlet of the first sedimentation cell, which had accumulated the greatest thickness of ochre (Fig. 1). Analyses were limited to the ochre portion of the sediment column.

2.2. Pore Water Samples

An aliquot of the pore water was allowed to warm to room temperature for pH and Eh measurements using an Orion pH electrode and a Corning combination redox electrode with a Pt-sensing element and a Ag/AgCl reference element. The remainder of the pore water was filtered using a 0.2-μm polypropylene syringe filter and split into two subsamples, one of which was acidified with approximately 1 mL of ultra-pure 6 *M* HCl/100 mL of sample for measurement of dissolved metals. The other subsample was not acidified and was used for SO_4 analysis with a Dionex ion chromatograph. Total concentrations of Al, Ca, Mg, Mn, Na, and K in the pore waters sampled in 2000 were measured using a Perkin-Elmer Optima 3000 inductively coupled plasma optical emission spectrometer (ICP-OES). Ferrous and total dissolved Fe (Fe_t) (following reduction with hydroxylamine hydrochloride) were measured colorimetrically by the ferrozine technique (To et al., 1999). A similar procedure was followed for the 1996 samples except that the Fe_t was measured by ICP-OES and other metals were not analyzed.

2.3. Solid Samples

Solid samples were freeze dried, and total C and S were determined by combustion using a CE instruments NC 2100 soil analyzer and a LECO Model 521 induction furnace, respectively. Total Fe, Al, Ca, Mg, Mn, Na, and K in the solids were determined by selective dissolution of a 100-mg sample in 20 mL of ultra-pure 6 *M* HCl for a period of 48 h (Winland et al., 1991). The acid solutions were then centrifuged for 10 min at 1010 RCF, the supernatants were removed and analyzed by ICP-OES, and the acid insoluble residues were quantified gravimetrically. The oxalate-extractable Fe fraction was measured by reacting 50-mg samples with 40 mL of 0.2 *M* ammonium oxalate (pH 3) (McKeague and Day, 1966). The samples were shaken in the dark for 4 h, centrifuged for 10 min at 1010 RCF, and Fe in the supernatant was quantified by atomic absorption spectroscopy.

The mineralogical composition of the precipitates was evaluated by X-ray diffraction (XRD) analysis of randomly oriented powder samples using CuKα radiation and a Phillips PW 1316/90 diffractometer equipped with a θ-compensating slit, a 0.2-mm receiving slit, and a diffracted-beam monochromator (Brady et al., 1986). Freeze-dried samples were scanned from 3 to 80° 2θ using a step interval of 0.01° 2θ and a counting time of 4 s. Fourier-transform infrared (FTIR) absorption spectra were recorded with a Mattson Instruments spectrophotometer using powdered samples diluted to 2.5 wt.% in KBr (Carlson et al., 2002). Diffuse reflectance spectra were collected from 150–1500 cm^{-1} as the average of 300 sample scans at 1 cm^{-1} resolution. Selected sediment samples were gold coated to improve conductivity and examined with a Phillips XL30 scanning electron microscope (SEM). Uncoated samples were analyzed using an energy-dispersive X-ray spectrophotometer (EDS) for chemical analysis.

Specific surface area was determined with a Micromeritics Flowsorb II 2300 surface area analyzer (Carlson et al., 2002). Approximately 75–100 mg of sediment was placed in a sample holder, dried over P_2O_5 for 48 h, and analyzed by the single-point Brunauer-Emmett-Teller method using N_2 as the absorbate.

Color determinations were performed on dry, homogeneously ground samples using a Minolta CR-300 Chroma Meter with standard illuminant C (Post et al., 1993). The measuring probe was rested in a vertical position on the sample and a xenon arc lamp was used to measure light reflected from the sample in the visible portion of the spectrum. Data were reported as an average of three readings using Munsell color notation.

Table 1. Properties of sediment solids.

Depth from surface (cm)	Color		Carbon % solid		Acid insoluble residue % solid		Density (D_b) (g/cm^3)	Surface Area (m^2/g)
	1996	2000	1996	2000	1996	2000	2000	2000
1.5	8.4YR3.7/5.0	8.1YR3.7/5.8	0.7	0.6	4	0	0.29	16
4.5	7.8YR3.8/5.7	8.3YR4.2/6.4	0.4	0.7	1	0	0.50	63
7.5	8.4YR4.5/6.8	9.0YR5.0/7.8	0.3	0.6	2	0	0.44	79
10.5	8.6YR4.6/7.5	9.5YR5.5/8.5	0.3	0.6	3	4	0.41	127
13.5	8.8YR5.3/8.2	9.4YR5.4/8.7	0.3	0.4	2	1	0.43	170
16.5	8.8YR5.1/8.1	9.5YR5.4/8.6	0.3	0.5	4	0	0.40	150
19.5	9.1YR5.2/8.2	0.1Y5.8/7.9	0.3	0.7	4	1	0.40	137
22.5	9.1YR5.4/7.4	9.3YR5.2/8.4	0.6	0.6	1	1	0.46	139
25.5	9.3YR5.4/7.8	9.3YR5.3/8.6	0.6	0.5	10	3	0.47	177
28.5	9.1YR5.3/7.5	0.1Y5.8/8.5	2.4	0.6	15	9	0.40	140
31.5	8.9YR5.4/8.0	9.6YR5.5/8.9	1.3	0.9	15	4	0.29	120

D_b = dry bulk density.

Table 2. Major and minor element composition[a] of the solid phase for samples collected in 1996 and 2000.

Depth from surface (cm)	Fe		S		Al		Ca		Mg		Mn		Na		K	
	1996	2000	1996	2000	1996	2000	1996	2000	1996	2000	1996	2000	1996	2000	1996	2000
	(g/kg)								(mg/kg)							
1.5	534	552	74	61	1590	1213	797	519	181	65	93	78	221	192	182	216
4.5	551	553	65	55	951	1788	767	635	159	41	86	79	182	174	505	*
7.5	569	596	61	40	889	1280	700	633	121	50	89	85	*	67	*	*
10.5	598	634	56	28	952	915	761	577	182	64	95	85	68	193	270	*
13.5	576	606	50	25	668	969	713	654	75	56	87	85	68	206	*	*
16.5	613	591	45	24	720	1166	933	697	168	106	94	86	50	35	*	*
19.5	617	484	38	20	627	1869	828	853	202	216	89	93	19	*	*	319
22.5	530	601	31	22	2140	1293	893	820	358	44	115	82	*	*	*	334
25.5	630	595	22	22	2868	1600	2464	906	376	90	116	86	270	48	*	143
28.5	558	628	14	19	13091	3634	13511	1053	2021	132	244	95	*	329	384	429
31.5	554	597	18	11	6928	6201	22893	1023	1676	53	270	120	22	19	*	*

[a] Concentrations corrected for water content (110°C) and acid insoluble residue.
* Concentration in acid extract was below detection limit.

3. RESULTS AND DISCUSSION

3.1. Wetland Properties and Sedimentation Rates

The Carbondale wetland was commissioned in 1990, and both discharge and influent drainage quality were monitored in two year-long studies beginning in April 1991 (Sritharan et al., 1992) and February 1999 (Shimala, 2000). Drainage entering the wetland had pH values ranging from 3.5 to 4.5 and average Fe and SO_4 concentrations of 110 and 1400 mg/L, respectively, and did not change appreciably over time. Iron removal effi-

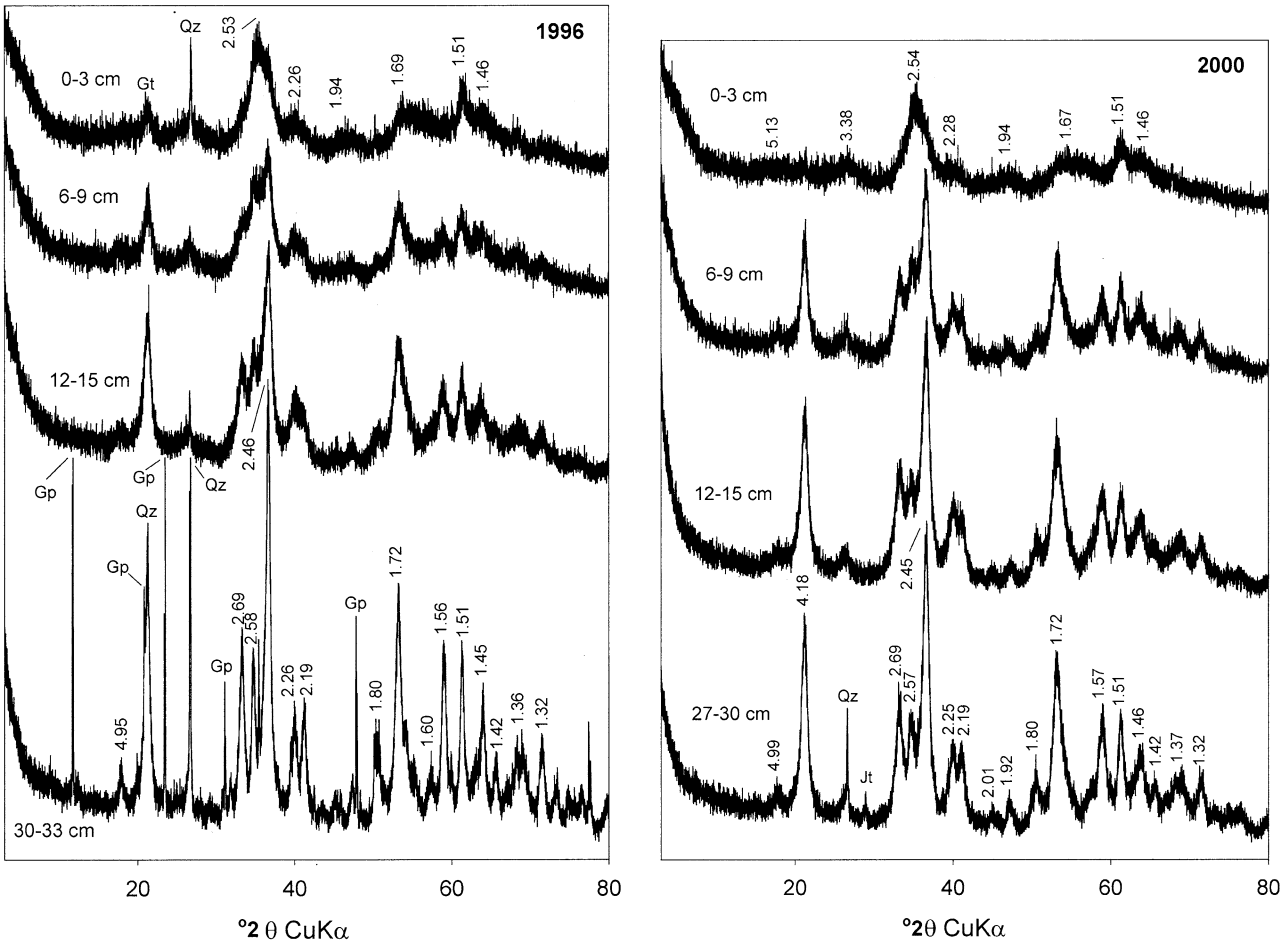

Fig. 2. X-ray powder diffraction patterns for samples at various depths below the sediment surface in 1996 and 2000. Gp = gypsum; Gt = goethite; Jt = jarosite; Qz = quartz. d-spacings are in Å.

ciency decreased slightly from 1991 to 2000, but was consistently greater than 60%. Removal rates for SO_4, Al, and Mn were much lower than Fe, and pH decreased from inlet to outlet.

Flow rate into the main wetland system ranged from 6 to 9 L/s, with significant losses due to seepage into the groundwater. Residence time was calculated to be 4 d using the reservoir volume and inflow rate (Sritharan et al., 1992), but was measured at 7.4 h using a tracer technique in April 2000 (Shimala, 2000). This deviation between the calculated and actual residence time was likely due to the general failure of the plant cover, increased sediment level, preferential flow, and channeling through collapsed tunnels burrowed by animals (Shimala, 2000).

Maximum deposition of ochre during the first decade of operation occurred in the first cell. Cores collected in September 1996, showed an accumulation of approximately 33 cm of sediment, which essentially filled the first basin. Dry densities measured in 2000 ranged from 0.29 to 0.50 g/cm^3 and averaged 0.41 g/cm^3 (Table 1). If similar densities were applied to the 1996 core, a deposition rate of 64 g/m^2/d over the first 6 yr can be calculated. Assuming an average Fe content of 585 g/kg (Table 2), this rate would correspond to 37 g Fe/m^2/d. Lower densities would yield rates more similar to the 20 g Fe/m^2/d reported by Hedin et al. (1994). Minimal sedimentation occurred after 1996 due to channeling of drainage away from the sampling site (Fig. 1).

The sediment cores in both years were collected from a stable area (uneroded) with a crusty, aggregated surface layer (0–6 cm) that became more fine-grained and loose with depth. The color graded from reddish brown at the surface to yellowish brown at the base, with no distinct stratification (Table 1). The 1996 core tended to be darker red in the upper 18 cm (average hue of 8.5 YR) than that collected in 2000 (average hue of 9.0 YR). Total C contents were greater at most depths in the 2000 core but were generally small (<0.75%) in both cores (Table 1). The solid phase was composed almost entirely of ochreous precipitates with minor acid insoluble residue (Table 1).

3.2. Solid-phase Mineralogy

The upper 6–9 cm of the sediment column in both collection years was composed primarily of schwertmannite, which is a poorly ordered oxyhydroxysulfate that commonly forms in mine drainage waters with pH in the range of 2.8–4.5 and sulfate concentrations ranging from 1000–3000 mg/L (Bigham et al., 1992). X-ray patterns displayed the eight broad peaks typical for schwertmannite with additional weak reflections indicating trace amounts of goethite and/or quartz (Fig. 2). Chemical analyses indicated an Fe/S mole ratio of 5.0 that corresponded to the formula $Fe_8O_8(OH)_{4.8}(SO_4)_{1.6}$, which is within the range considered typical for schwertmannite (Bigham et al., 1996). Infrared spectra from the surface samples were dominated by absorption bands due to υ_1 (SO_4) at 970 cm^{-1}, υ_4 (SO_4) at 610 cm^{-1}, and a splitting of the υ_3 fundamental of SO_4 to yield features at 1210, 1130, and 1040 cm^{-1} (Fig. 3). These bands, along with a band at 700 cm^{-1}, result from OH-stretching and have been shown to be typical of schwertmannite (Bishop and Murad, 1996). Scanning electron microscope examinations and EDS analyses of the surface samples revealed Fe- and S-rich spheres ranging in size from 1–2 μm (Figs. 4a and 5a). The "pincushion" morphology was

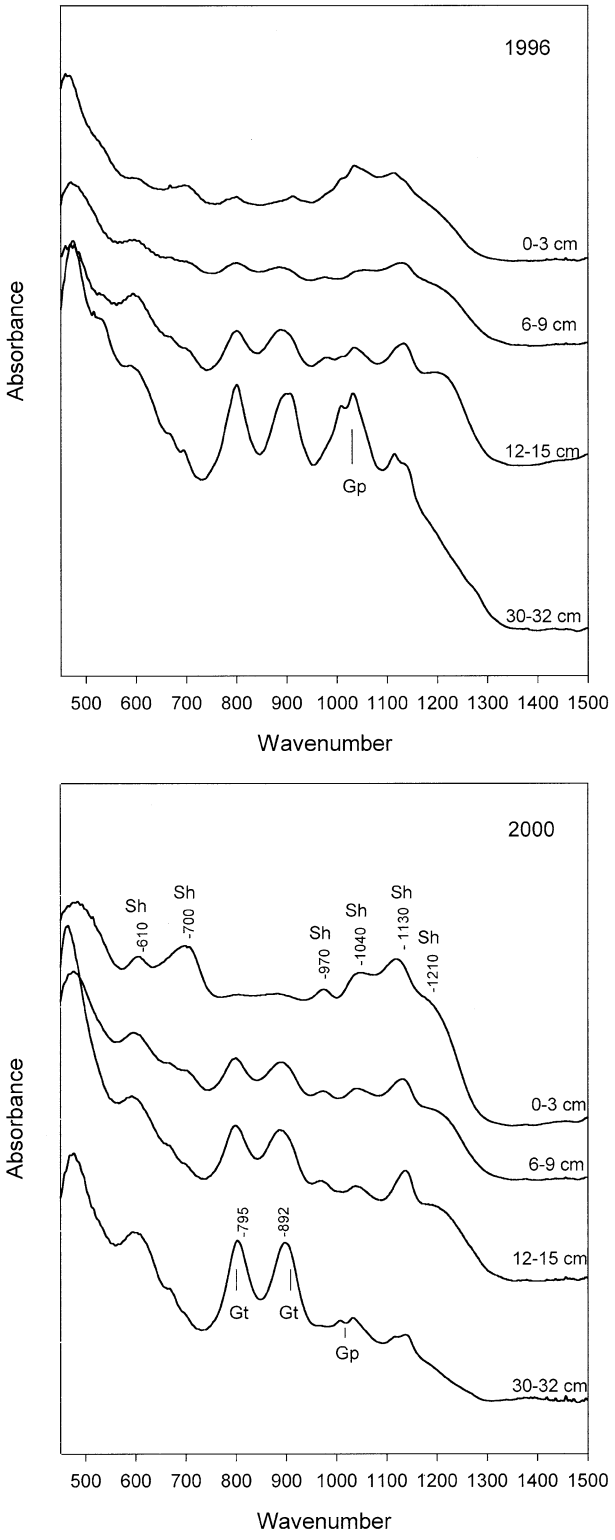

Fig. 3. Infrared spectra for samples at various depths below the sediment surface in 1996 and 2000. Gp = gypsum; Gt = goethite; Sh = schwertmannite.

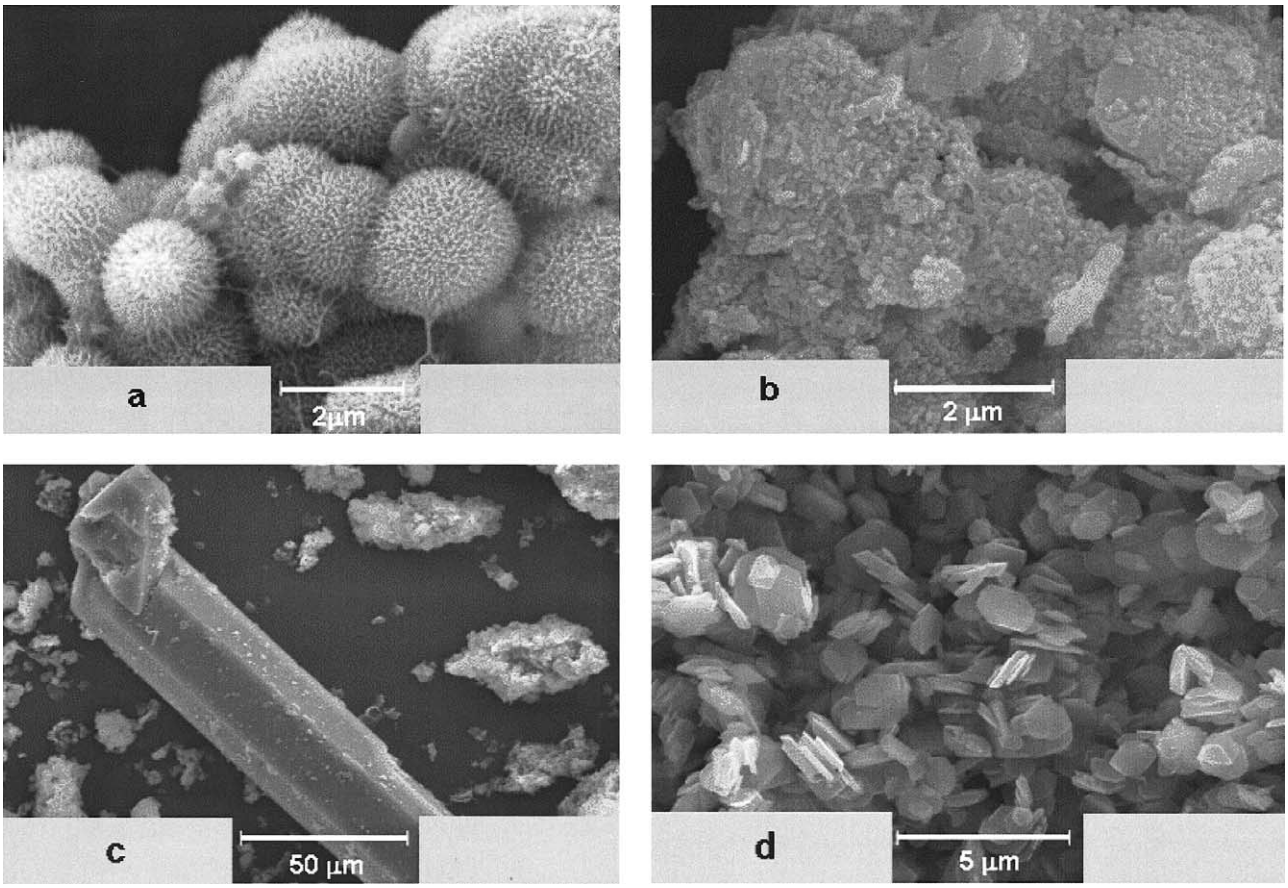

Fig. 4. Scanning electron microscope images of (a) schwertmannite (0–3 cm), (b) goethite (30–33 cm), (c) gypsum (30–33 cm), and (d) jarosite (25–30 cm) from the Carbondale wetland.

similar to that previously described for synthetic schwertmannite with smaller spheres ranging from 0.1–0.2 μm in diameter (Bigham et al., 1990). Schwertmannite from the 0–3 cm depth was densely aggregated, probably due to periodic drying. Aggregation may have accounted for the reddish-brown color and small specific surface area (Table 1) as compared to synthetic specimens with surface areas that usually exceed 200 m^2/g. The actual surface area of the Carbondale schwertmannite was presumably underestimated because internal surfaces were not accessible to N_2 (Carlson and Schwertmann, 1981).

The dominant mineral phase at the bottom of both sediment columns (33 cm) was goethite. SEM observations indicated that the average diameter of the goethite particles was ~0.15 μm (Fig. 4b), and this small particle size was reflected in specific surface areas exceeding 100 m^2/g (Table 1). IR spectra also had characteristic absorption bands at 892 and 795 cm^{-1}, corresponding to the δ-OH and γ-OH bending vibrations in goethite (Cornell and Schwertmann, 1996). Samples collected from the bottom of the sediment column in 1996 were shown by XRD, FTIR, and EDS analysis to contain gypsum ($CaSO_4 \cdot 2H_2O$) (Figs. 2, 3, and 5c) in addition to goethite. Presumably, dissolution of carbonates in the compost material or limestone at the base of the wetland cell released sufficient Ca into the pore water to induce gypsum precipitation in the form of large, lath-like crystals (Fig. 4c). Chemical analysis of the solids for Ca indicated gypsum contents ranging from 6 to 10 wt.% in the lower 6 cm (Table 2). The lack of detectable gypsum in XRD patterns from samples collected at similar depths in 2000 was likely due to a depletion of carbonates over time, thus lowering Ca concentrations in solution, and resulting in conditions favorable for gypsum dissolution.

Although little gypsum was present in the 2000 core, total S content of the solid phase was slightly elevated in the 25.0–28.5 cm zone compared to the 1996 samples (Table 2). This increase coincided with a region where the sediment was most yellow (Table 1) and where nodules of jarosite [$(K,Na)Fe_3(SO_4)_2(OH)_6$] were found (Fig. 6a). The nodules were approximately 5 mm in diameter, and SEM observations showed a hexagonal, plate-like morphology for the jarosite crystals (Fig. 4d). EDS spectra (Fig. 5d) and analyses following dissolution of the jarosite in 6 *M* hydrochloric acid (data not given) showed the jarosite contained mostly K (4.0 wt.%) with some Na (0.8 wt %) as the monovalent cation. The nodules also yielded 26 wt.% acid insoluble residue. X-ray diffraction analysis of the residue revealed mostly clay minerals, including illite, which likely provided a source of K for jarosite formation (Ross et al., 1982) (Fig. 6b).

The middle portions of both sediment columns (6–24 cm) represented a transition zone where the proportion of schwertmannite decreased as goethite increased with depth. XRD patterns contained peaks for both schwertmannite and goethite, and the goethite exhibited line broadening indicative of poor

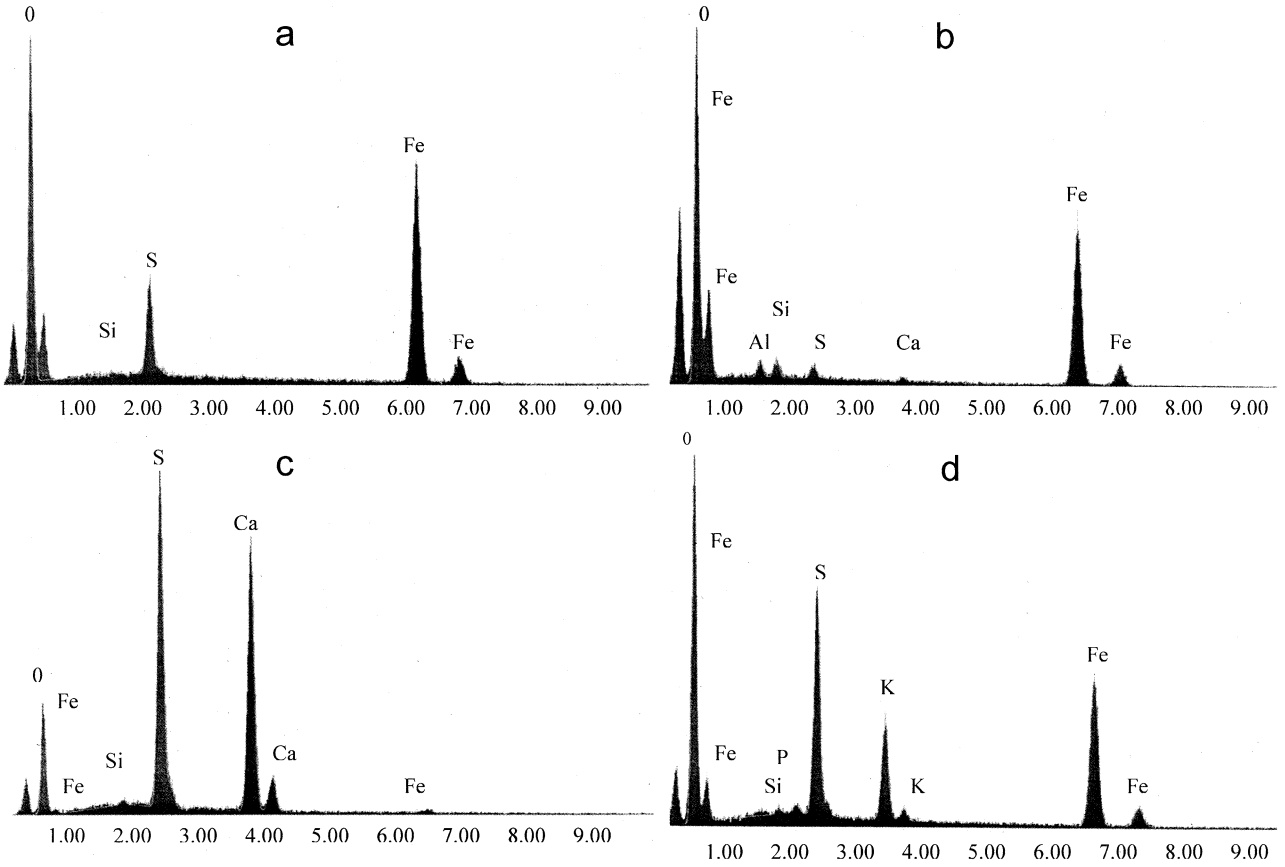

Fig. 5. Energy dispersive X-ray spectra of (a) schwertmannite (0–3 cm), (b) goethite (30–33 cm), (c) gypsum (30–33 cm), and (d) jarosite (25–30 cm) from the Carbondale wetland.

ordering compared to that occurring at the base of the ochre column (Fig. 2). The two OH bending vibrations of goethite became more intense with depth as bands characteristic of SO_4 diminished (Fig. 3). Likewise, total solid-phase S decreased with depth (Table 2). These data support previous laboratory (Bigham et al., 1996; Desborough et al., 2000) and field studies (Peine et al., 2000) that indicated schwertmannite was a metastable precursor to goethite.

The depth distribution of schwertmannite and goethite was quantified and conversion rates estimated using samples extracted in the dark with acid (pH 3) ammonium oxalate to selectively dissolve schwertmannite and leave goethite as a mostly insoluble residue. The acid ammonium oxalate procedure was developed for the selective removal of ferrihydrite from soils with recommended extraction times ranging from 2 to 4 h (Schwertmann, 1964; McKeague and Day, 1966). Brady et al. (1986) and Dold (2003) observed that schwertmannite can be dissolved in as little as 15 min, but schwertmannite in the Carbondale sediments was found to be more recalcitrant, perhaps due to its highly aggregated nature. Therefore, an extraction time of 4 h was defined in preliminary experiments by incrementally increasing the extraction time until XRD confirmed the residues were free of schwertmannite. The oxalate-extractable Fe was then converted to % schwertmannite by using the formula weight defined previously, and goethite contents were obtained by difference. Estimates obtained by this procedure were also confirmed by XRD analysis of binary mixtures of schwertmannite and goethite (Klug and Alexander, 1954). The mixtures were prepared from samples taken at 0–3 cm and 30–33 cm depths in the 2000 core.

In the 1996 samples, schwertmannite decreased from almost 100 wt.% at the sediment surface to 10 wt.% at the base of the sediment column, whereas goethite increased from 5–80 wt.% (Fig. 7). Assuming that 1) all goethite was produced by transformation of schwertmannite and 2) active deposition of schwertmannite was still occurring, the minimum conversion rate for schwertmannite to goethite during the period 1990–1996 was calculated as 30 mol/m^3/yr. Except for the surface 6 cm, schwertmannite was more abundant at all depths in 1996 as compared to 2000, which indicated that conversion continued after active sedimentation had ceased (Fig. 7). As a whole, the sediment column collected in 1996 contained 7% more schwertmannite than samples analyzed in 2000, suggesting a slower conversion rate of approximately 10 mol/m^3/yr. The persistence of schwertmannite at the surface of the sediment could have reflected active Fe cycling between dissolved and precipitated phases with constant replenishment of schwertmannite in the capillary fringe of the sediment column. Alternatively, the dense aggregation, low exposed surface area (Table 1), and oxic conditions could have prevented dissolution of schwertmannite.

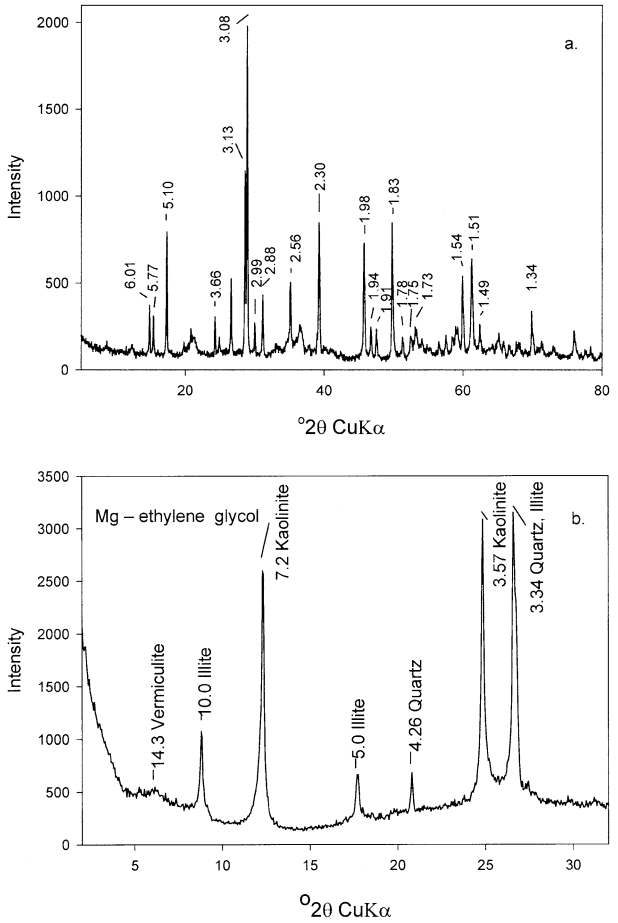

Fig. 6. X-ray diffraction patterns for (a) jarosite and the associated (b) acid insoluble residue in nodules isolated from a depth of 25–30 cm in the 2000 sediment core. d-spacings are in Å.

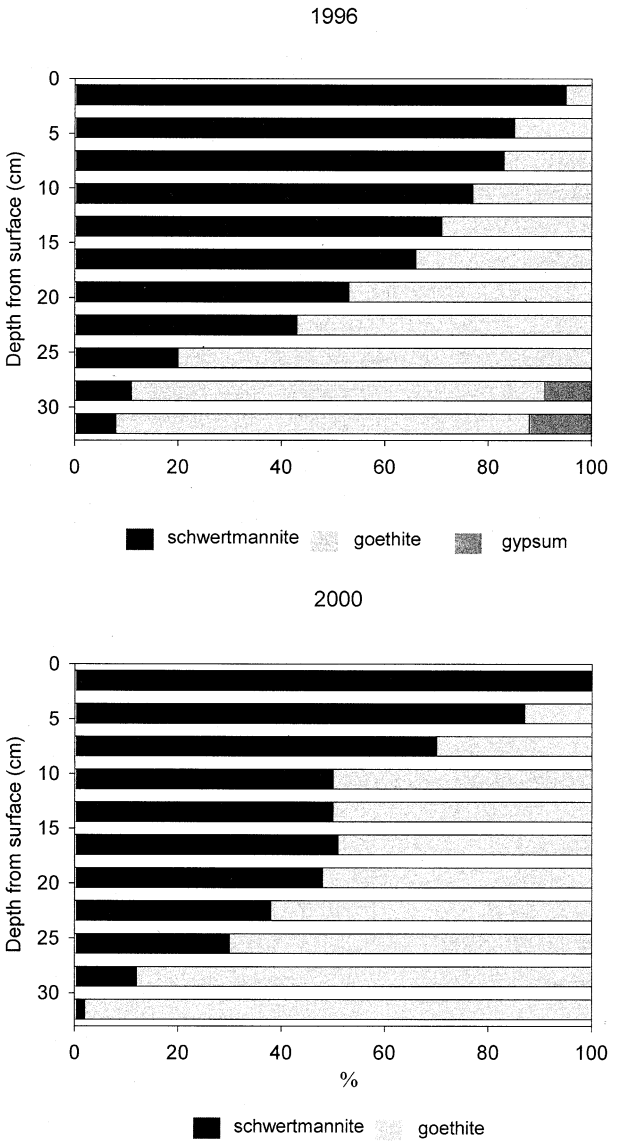

Fig. 7. Depth distributions of schwertmannite, goethite, and gypsum from the 1996 sediment core and schwertmannite and goethite from the 2000 sediment core.

3.3. Pore Water pH, Eh, Fe, and SO_4

Pore water samples from 1996 and 2000 showed striking spatial and temporal differences in pH (Fig. 8A). In 1996, pH decreased in the upper half of the sediment column from 2.6 to 2.0 and then increased to 6.2 at the bottom. In 2000, the surface pH was greater and increased less with depth from 3.4 to 4.4. Increased pH toward the bottom of the sediment column was expected in both years due to influence of the limestone layer. In addition, the activity of sulfate-reducing bacteria in compost underlying the ochre, as indicated by the odor of H_2S, may have contributed to increases in pH through the production of bicarbonate. Over time, dissolution or armoring of the limestone decreased the neutralizing capacity and resulted in less dramatic increases in pH with depth for the 2000 sampling. Lower pore water pH at the sediment surface in 1996 compared to the influent drainage (pH 3.6) was likely due to active iron precipitation through oxidation and hydrolysis. By the 2000 sampling, flow of drainage water was channeled, which decreased the rates of iron precipitation in most areas of the first cell. Thus, the pH of pore water at the top of the sediment was similar to the influent drainage. Decreased pH in the upper portion of the sediment column in 1996 corresponded with the observed mineralogical transformation of schwertmannite to goethite, which releases protons (reaction 1) (Bigham et al., 1996).

$$Fe_8O_8(OH)_{4.8}(SO_4)_{1.6(s)} + 3.2\ H_2O_{(l)} \rightarrow 8\ FeOOH_{(s)} + 3.2\ H^+_{(aq)} + 1.6\ SO^{2-}_{4(aq)} \quad (1)$$

Sulfate is also released when schwertmannite is converted to goethite, which was clearly demonstrated in the samples collected in 1996. Sulfate concentrations in the pore water increased from 1010 mg/L near the sediment surface to 4630 mg/L at 25.5 cm depth. Assuming a bulk density (D_b) of 0.4 g/cm^3, a particle density (D_p) of 4.4 g/cm^3, and 90% porosity [$1-(D_b/D_p)$], the decay of only 1.5 g of schwertmannite/100 cm^3 of sediment would increase the sulfate concentration by over 3000 mg/L above background. Below 26 cm, the SO_4

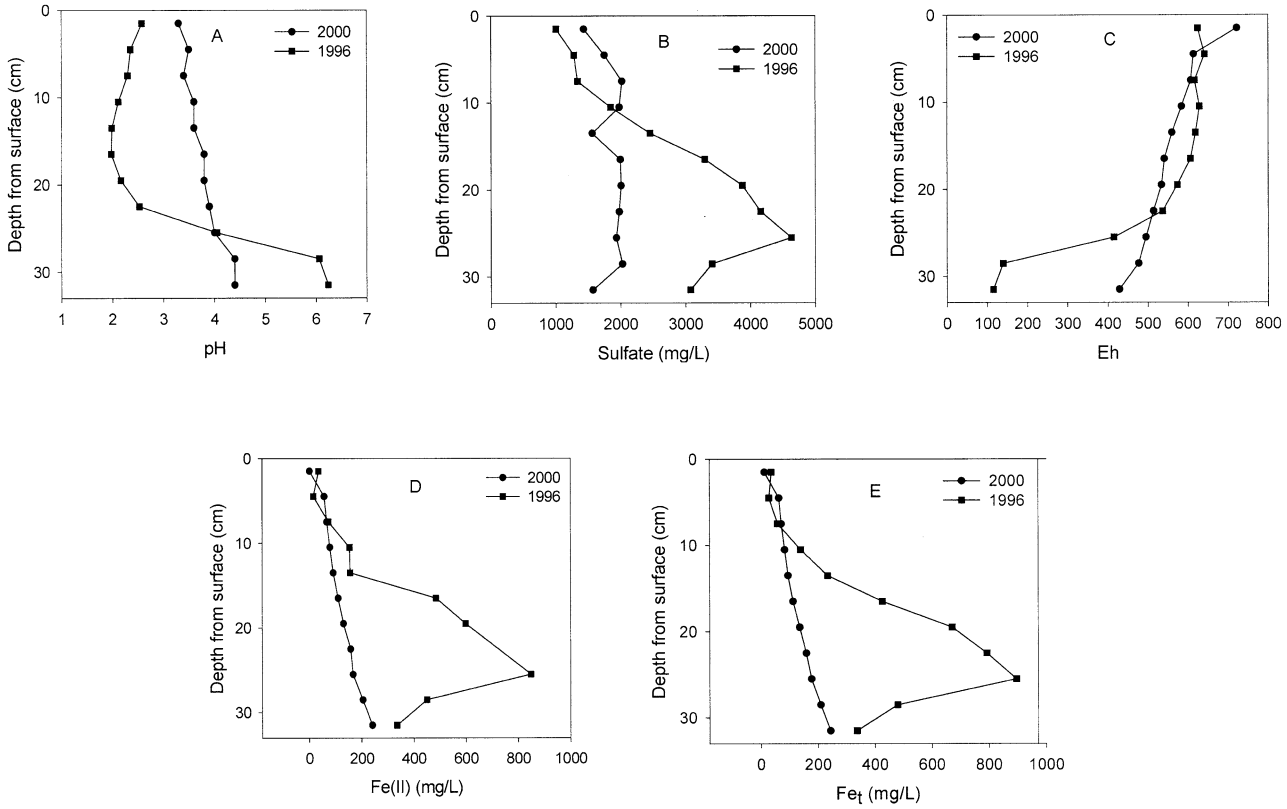

Fig. 8. Pore water (A) pH, (B) sulfate, (C) Eh, (D) Fe(II), and (E) Fe_t for samples collected in 1996 and 2000.

concentration decreased to 3070 mg/L (Fig. 8B). In 1996 this decreased sulfate was mostly due to the precipitation of gypsum, but may also have involved sulfate-reducing bacteria and loss of sulfide to the atmosphere as H_2S or to solids through precipitation as FeS (sulfides were detected in compost beneath the ochre). Sulfate concentrations in pore water samples collected in 2000 showed no distinct gradients with depth but varied from 1420 mg/L to 2030 mg/L (Fig. 8B and Table 3). These results indicated a much less dynamic system.

The Eh of pore water samples collected from the upper half of the sediment column in 1996 ranged from 605 mV to 642 mV and then decreased sharply with depth to 115 mV (Fig. 8C). In 2000, Eh gradually decreased with depth from 776 to 429 mV. Lower Eh with depth was expected due to the consumption of O_2 diffused from the surface; however, the lower Eh near the bottom of the sediment column in 1996 may have also resulted from greater microbial activity. The compost material in 1996 presumably had more biodegradable electron donors for sulfate reduction as compared to 2000.

Total Fe and Fe(II) concentrations in 1996 showed depth trends similar to sulfate; both parameters increased with depth to 25.5 cm and then decreased (Fig. 8D–E). Total Fe ranged from 30 mg/L to 900 mg/L, with Fe(II) comprising 40–100% of the total. Ratios of Fe(II)/Fe_t that exceeded unity were

Table 3. Pore water composition for samples collected in 2000.

Depth from surface (cm)	Al	Ca	Fe_t	Fe(II)	K	Mg	Mn	Na	SO_4
					(mg/L)				
0	33.2	160.2	26.4	0.4	4.2	81.6	7.3	23.7	2688
1.5	38.1	159.0	12.0	1.6	4.4	81.8	7.2	23.8	1434
4.5	39.5	159.8	62.7	57.7	4.3	81.5	7.2	23.1	1753
7.5	37.2	167.8	71.0	67.2	4.4	83.9	7.3	24.0	2021
10.5	35.2	147.3	82.7	79.0	4.6	89.3	7.7	25.2	1978
13.5	32.0	190.0	94.2	91.5	5.0	90.5	7.5	25.1	1565
16.5	26.4	223.7	111.8	110.4	4.6	85.1	6.9	23.6	1996
19.5	20.0	249.3	135.3	130.7	5.6	82.8	6.7	23.1	2009
22.5	15.7	276.8	158.3	158.0	6.1	83.7	6.4	23.1	1979
25.5	12.8	293.4	176.5	167.0	7.4	84.4	6.3	23.0	1934
28.5	8.1	316.4	208.9	204.6	9.0	84.7	6.1	22.9	2027
31.5	5.1	334.0	242.8	241.1	11.8	86.6	6.1	23.4	1572

observed with some samples and have been reported in previous analyses of pore waters using the ferrozine method (e.g., Luther et al., 1996). The generally high dissolved Fe contents could be related to the fact that iron in poorly ordered schwertmannite was more susceptible to reduction than in relatively well ordered goethite (Münch and Ottow, 1980; Bigham et al., 1996). Moreover, high rates of Fe(III) reduction have recently been reported in acidic coal mine lakes (Blodau et al., 1998; Peine et al., 2000) where Küsel et al. (1999) demonstrated that the reduction of Fe(III)-hydroxides could be mediated by *Acidophilium* species. Thus, the observed distribution of dissolved Fe(II) in the sediment column may be related to the distribution of iron-reducing bacteria as well as the susceptibility of the iron precipitates to reduction.

In 2000, both Fe(II) and Fe_t increased with depth; however, the concentrations were much lower than in 1996 even though redox profiles were similar to 25 cm depth (Fig. 8C and Table 3). Total iron ranged from 12 mg/L near the surface to 290 mg/L near the bottom of the core, with the percentage of Fe(II) increasing with depth from 13 to 100%. Lower concentrations of iron in solution during 2000 could perhaps be attributed to the greater proportion of goethite relative to schwertmannite in these sediments and to the fact that goethite was less soluble than schwertmannite at comparable Eh values.

3.4. Al, Ca, Mg, Mn, Na, and K in the Solid and Pore Water Samples

Aluminum was the most abundant cation in the solid phase after Fe (Table 2). Precipitation of Al as $Al(OH)_3$ or a hydroxysulfate is pH dependent, with Al solubility decreasing above pH 4.5 (Nordstrom and Alpers, 1999). Thus, Al concentrations in the solid phase were at a maximum and those in the pore waters at a minimum near the bottom of the sediment column where pH was in the range of 4.5–6.0 (Tables 2 and 3). No Al minerals were detected in the solids due to low concentration or the poor structural order of any Al precipitates. Calcium content of the solids also increased with depth due to the precipitation of gypsum in the 1996 samples (Table 2), and was presumably coupled to elevated solution concentrations of Ca arising from the dissolution of carbonates in the wetland cell liner. Calcium concentrations in the solids were less in the 2000 samples (Table 2) due to the dissolution of gypsum, but the distribution of dissolved Ca still increased with depth (Table 3).

Solid-phase Mg and Mn in the 1996 samples increased with depth and were generally greater than in 2000 when both pore water and solid concentrations were relatively constant with depth. The Mg distribution probably reflected contributions from the compost or limestone. Sodium and K showed no distinct trends with depth in the solid phase for either sampling period except that K contents were elevated in the samples from 2000 over the depth increment where jarosite was found (Table 2). Solution K also showed some increase with depth in the 2000 samples (Table 3).

4. CONCLUSIONS

The Carbondale wetland examined in this study has served as a reservoir for iron precipitates from influent mine drainage. Drainage chemistry favored an initial accumulation of schwertmannite, which over time has partially transformed to goethite. The calculated rate of transformation has varied from 10–30 $mol/m^3/yr$. These rates demonstrate that the sediment column has not been a static system, and the instability of schwertmannite has had a significant impact on pore water chemistry through production of acidity and the release of Fe and SO_4. Trace metal cycling could also become an issue in systems with greater contaminant loads. High $Fe(II)/Fe_t$ ratios in the pore waters probably reflect the activity of acidophilic, Fe-reducing bacteria. Microbially mediated reduction of iron oxides under acidic conditions has rarely been reported and deserves further investigation because of the potential significance to many acid sulfate waters.

The compost and limestone added to the base of the wetland cells have functioned to partially neutralize the low pH drainage, and the compost has modified the redox potential through stimulation of anaerobic microbial decomposition and sulfate reduction. Both effects, however, have been spatially limited by diffusion and have mostly impacted the compost layer and sediment immediately adjacent to the compost. In addition, both effects diminished with time as reactive components were consumed.

Acknowledgments—We gratefully acknowledge the analytical assistance of Mr. D. Beak and Mr. U. Soto. Dr. O. H. Tuovinen provided helpful suggestions and a critical review of this manuscript. Funding for W.B.G. was provided by the NASA graduate student research program, grant 9-51. Additional salary support was provided by the DOD and by OSU-OARDC. Comments and suggestions by C. A. Cravotta, III, R. Capo, and an anonymous reviewer also rendered significant improvements in the manuscript.

Associate editor: P. A. Maurice

REFERENCES

Barton C. D. and Karathanasis A. D. (1999) Renovation of a failed constructed wetland treating acid mine drainage. *Environ. Geol.* **39,** 39–50.

Bigham J. M. and Nordstrom D. K. (2000) Iron and aluminum hydroxysulfates from acid sulfate waters. In *Sulfate Minerals—Crystallography, Geochemistry and Environmental Significance* (eds. C. N. Alpers, J. L. Jambor and D. K. Nordstrom) Miner. Soc. Am. Washington, D.C., *Rev. Miner. Geochem.* **Vol. 40,** pp. 351–403.

Bigham J. M., Schwertmann U., Carlson L., and Murad E. (1990) A poorly crystallized oxyhydroxysulfate of iron formed by bacterial oxidation of Fe(II) in acid mine waters. *Geochim. Cosmochim. Acta* **54,** 2743–2758.

Bigham J. M., Schwertmann U., and Carlson L. (1992) Mineralogy of precipitates formed by the biogeochemical oxidation of Fe(II) in mine drainage. In *Biomineralization Processes of Iron and Manganese—Modern and Ancient Environments* (eds. H. C. W. Skinner and R. W. Fitzpatrick), pp. 219–232. Catena Suppl. 21, Cremlingen-Destedt.

Bigham J. M., Schwertmann U., Traina S. J., Winland R. L., and Wolf M. (1996) Schwertmannite and the chemical modeling of iron in acid sulfate waters. *Geochim. Cosmochim. Acta* **60,** 2111–2121.

Bishop J. L. and Murad E. (1996) Schwertmannite on Mars? Spectroscopic analyses of schwertmannite, its relationship to other ferric minerals, and its possible presence in the surface material of Mars. In *Mineral Spectroscopy: A Tribute to Roger Burns* (eds. M. D. Dyar, C. McCommon, and M. W. Schaefer), pp. 337–358. Spec. Publ. 5, Geochem. Soc., Washington, D.C.

Blodau C., Hoffmann S., Peine A., and Peiffer S. (1998) Iron and sulfate reduction in the sediments of acidic mine lake 116 (Branden-

burg, Germany): Rates and geochemical evaluation. *Water Air Soil Pollut.* **108,** 249–270.

Brady K. S., Bigham J. M., Jaynes W. F., and Logan T. J. (1986) Influence of sulfate on Fe-oxide formation: Comparisons with a stream receiving acid mine drainage. *Clays Clay Min.* **34,** 266–274.

Carlson L., Bigham J. M., Schwertmann U., Kyek A., and Wagner F. (2002) Scavenging of As from acid mine drainage by schwertmannite and ferrihydrite: A comparison with synthetic analogues. *Environ. Sci. Technol.* **36,** 1712–1719.

Carlson L. and Schwertmann U. (1981) Natural ferrihydrites from Finland and their association with silica. *Geochim. Cosmochim. Acta* **45,** 421–429.

Cornell R. M. and Schwertmann U. (1996) *The Iron Oxides. Structure, Properties, Reactions, Occurrence and Uses*. VHC, Weinheim.

Desborough G., Leinz R., Sutley S., Briggs P., Swayze G. A., Smith K., and Breit G. (2000) Leaching studies of schwertmannite-rich precipitates from the Animas River headwaters, Colorado and Boulder River headwaters, Montana, U.S. Geol. Surv., Open file report. 00-004, 11 pp.

Dold B. (2003) Dissolution kinetics of schwertmannite and ferrihydrite in oxidized mine samples and their detection by differential X-ray diffraction (DXRD). *Appl. Geochem.* **18,** 1531–1540.

Hedin R. S., Nairn R. W., and Kleinmann R. L. P. (1994) Passive treatment of coal mine drainage: U.S. Bureau of Mines Information Circular IC 9389, 35 pp.

Hyman D. M. and Watzlaf G. R. (1997) Metals and other components of coal mine drainage as related to aquatic life standards. In *Proceedings of the 1997 National Meeting of the American Society for Surface Mining and Reclamation*, May 10–15, 1997, Austin, Texas. Princeton, W.V., American Society for Surface Mining and Reclamation, pp. 531–545.

Karathanasis A. D. and Thompson Y. L. (1995) Mineralogy of iron precipitates in a constructed acid mine drainage wetland. *Soil Sci. Soc. Am. J.* **59,** 1773–1781.

Klug H. and Alexander L. (1954) *X-ray Diffraction Procedures*. Wiley and Sons, New York, 716 pp.

Küsel K., Dorsch T., Acker G., and Stackebrandt E. (1999) Microbial reduction of Fe(III) in acidic sediments: Isolation of *Acidiphilium cryptum* JF-5 capable of coupling the reduction of Fe(III) to the oxidation of glucose. *Appl. Environ. Microbiol.* **65,** 3633–3640.

Luther W. G., III, Kostke J. E., Sulzberger B., and Stumm W. (1996) Dissolved organic Fe(III) and Fe(II) complexes in salt marsh porewaters. *Geochem. Cosmochim. Acta* **60,** 951–960.

McKeague J. A. and Day J. H. (1966) Dithionite- and oxalate-extractable Fe and Al as aids in differentiating various classes of soils. *Can. J. Soil Sci.* **46,** 13–22.

Münch J. C. and Ottow J. C. (1980) Preferential reduction of amorphous to crystalline iron oxides by bacterial activity. *Soil Sci.* **129,** 15–21.

Nordstrom D. K. and Alpers C. N. (1999) Geochemistry of acid mine waters. In *The Environmental Geochemistry of Mineral Deposits. Part A, Processes, Methods and Health Issues* (eds. G. S. Plumlee and M. J. Logsdon) *Rev. Econ. Geol*. **Vol. 6A,** pp. 133–160.

Peine A., Tritschler A., Küsel K., and Peiffer S. (2000) Electron flow in an iron-rich acidic sediment—evidence for an acidity-driven iron cycle. *Limnol. Oceanogr.* **48,** 1077–1087.

Post D. F., Bryant R. B., Batchily A. K., Huete A. R., Levine S. J., Mays M. D., and Escadafal R. (1993) Correlations between field and laboratory measurements of soil color. In *Soil Color* (eds. J. M. Bigham and E. J. Coilkosz), pp. 35–49. Spec. Publ. No. 31, Soil Sci. Soc. Am., Madison, WI.

Rose A. W. and Cravotta C. A., III. (1998) Geochemistry of coal-mine drainage. In *Coal Mine Drainage Prediction and Pollution Prevention in Pennsylvania: Harrisburg, PA* (eds. K. B. C. Brady, M. W. Smith and J. Schueck), pp. 1.1–1.22. Pennsylvania Department of Environmental Protection, 5600-BK-DEP2256.

Rose S. and Ghazi A. M. (1997) Release of sorbed sulfate from iron oxyhydroxides precipitated from acid mine drainage associated with coal mining. *Environ. Sci. Technol.* **31,** 2136–2140.

Ross G. J., Ivarson K. C., and Miles N. M. (1982) Microbial formation of basic ferric sulfates in laboratory systems and in soils. In *Acid Sulfate Soils* (eds. J. A. Kittrick, D. S. Fanning, and L. R. Hossner), pp. 77–95. Spec. Publ. No. 10, Soil Sci. Soc. Am., Madison, WI.

Schwertmann U. (1964) Differenzierung der Eisenoxide des Boden durch photochemische Extraktion mit sauer ammoniumoxalat-lösung. *Zeit. Pflanzenaern. Dung. Bodenkunde* **105,** 194–202.

Shimala J. R. (2000) Hydrogeochemical characterization of the Carbondale wetland, Athens County, Ohio: Evaluation of acid mine drainage remediation alternatives. M.S. thesis, Ohio University. 319 pp.

Skousen J. G., Rose A. W., Geidel G., Foreman J., Evans R., Hellier W., and others. (1998) *Handbook of Technologies for Avoidance and Remediation of Acid Mine Drainage*. Morgantown, W.V., National Mine Land Reclamation Center, 131 pp.

Sritharan S. I., Lowell C. A., and Beach K. (1992) *Wetland Monitoring: A Case Study in Carbondale, OH*. Field guide, Ohio Dept. Nat. Res., Columbus, OH. 11 pp.

To T. B., Nordstrom D. K., Cunningham K. M., Ball J. W., and McCleskey R. B. (1999) New method for the direct determination of dissolved Fe(III) concentration in acid mine waters. *Environ. Sci. Technol.* **33,** 807–813.

Webster J. G., Swedlund P. J., and Webster K. S. (1998) Trace metal adsorption onto an acid mine drainage(III) oxy hydroxy sulfate. *Environ. Sci. Technol.* **32,** 1361–1368.

Winland R. L., Traina S. J., and Bigham J. M. (1991) Chemical composition of ochreous precipitates from Ohio coal mine drainage. *J. Environ. Qual.* **20,** 452–460.